

Comparison of Detrending Methods in Spectral Analysis of Heart Rate Variability

Liping Li, Changchun Liu, Ke Li and Chengyu Liu

Abstract—Non-stationary trend in R-R interval series is considered as a main factor that could highly influence the evaluation of spectral analysis. It is suggested to remove trends in order to obtain reliable results. In this study, three detrending methods, the smoothness prior approach, the wavelet and the empirical mode decomposition, were compared on artificial R-R interval series with four types of simulated trends. The Lomb-Scargle periodogram was used for spectral analysis of R-R interval series. Results indicated that the wavelet method showed a better overall performance than the other two methods, and more time-saving, too. Therefore it was selected for spectral analysis of real R-R interval series of thirty-seven healthy subjects. Significant decreases ($19.94 \pm 5.87\%$ in the low frequency band and $18.97 \pm 5.78\%$ in the ratio ($p < 0.001$)) were found. Thus the wavelet method is recommended as an optimal choice for use.

Keywords—empirical mode decomposition, heart rate variability, signal detrending, smoothness priors, wavelet

I. INTRODUCTION

HEART rate variability (HRV) described as beat-to-beat variation in heart rate is an effective noninvasive method to assess the function of autonomic nervous system or to diagnose various pathologic changes of cardiovascular system[1]–[5]. A large number of methods are available for quantification of HRV, in which the spectral analysis is one of the most frequently used.

In spectral analysis, the spectrum of the R-R interval series is usually divided into several frequency bands, known as the very low frequency (VLF:0-0.04Hz), the low frequency (LF:0.04-0.15Hz) and the high frequency (HF:0.15-0.4Hz) bands[1]. The LF band is believed to be associated with the sympathetic and parasympathetic tone whereas the HF band is associated with the parasympathetic activity. The ratio of the LF and HF bands has been used as a measurement of sympathovagal balance[1]–[5]. As the successive R-R intervals are a series of data points sampled unevenly in time, and the resampling procedure might add the LF band and reduce the HF band[6], thus, the Lomb-Scargle (L-S) periodogram, a spectral method for unevenly sampled data[7],[8], was supposed more appropriate for spectral analysis in HRV[6]–[9].

As the presence of slow or irregular trends in the data series can potentially distort spectral analysis and lead to misinterpretations[2], several methods were used to remove the

non-stationary trends of the R-R interval series. Routine methods are usually based on first order or high order polynomial models[10],[11]. In 2002, M. Tarvainen developed a method based on smoothness prior approach (SPA)[12]. It operates like a time-varying FIR high pass filter and is simple to use. In 2006, R.Thuraisingham concluded that the wavelet method provided encouraging results in preprocessing of HRV[13]. The empirical mode decomposition (EMD) method was used for detrending in HRV by P. Flandrin *et al.* in 2004[14], which is regarded as a new automatic approach of removing non-stationary trend. It is difficult to determine the most suitable detrending method in real R-R interval series. In this study, four types of trends were proposed to simulate the trends in R-R interval series. The SPA, the wavelet and the EMD method were compared to detrend the artificial R-R interval series. L-S periodogram was used for spectral analysis and assessment of the detrending methods.

II. DATA ACQUISITION

A. Artificial R-R Interval Series

In this study, McSharry's model[15] was applied to simulate the artificial R-R interval series. In this model, a time series is generated following the real R-R interval series in mean, standard deviation and spectral characteristics. The spectral characteristics of the R-R interval series, including both the LF and HF bands, are replicated by specifying a bi-modal spectrum composed of the sum of two Gaussian functions as in (1), in which, f_{LF} and f_{HF} are the central frequency of the LF and HF bands, and c_{LF} , c_{HF} are the standard deviation of each band. Power in the LF and HF bands are given by P_{LF} and P_{HF} respectively, yielding an LF/HF ratio of $\alpha = P_{LF} / P_{HF}$.

$$S(f) = \frac{P_{LF}}{\sqrt{2\pi c_{LF}^2}} \exp\left(-\frac{(f - f_{LF})^2}{2c_{LF}^2}\right) + \frac{P_{HF}}{\sqrt{2\pi c_{HF}^2}} \exp\left(-\frac{(f - f_{HF})^2}{2c_{HF}^2}\right) \quad (1)$$

Then a time series $T(t)$ with power spectrum $S(f)$ is generated by taking the inverse Fourier transform of a sequence of complex numbers with amplitudes $\sqrt{S(f)}$ and phases which are randomly distributed between 0 and 2π . As in Fig.1 (a), an artificial R-R interval series with a length of 300 was generated by this model with a selection of the parameters as $f_{LF}=0.1\text{Hz}$, $f_{HF}=0.25\text{Hz}$, $c_{LF}=c_{HF}=0.01\text{Hz}$, $\alpha=0.5$.

This work is supported by the National High Technology Research and Development Program of China (863 Program) (No. 2009AA02Z408).

Changchun Liu is with the Institute of Biomedical Engineering, Shandong University, P. R. China. (e-mail: changchunliu@sdu.edu.cn).

B. Real R-R Interval Series

Thirty-seven healthy subjects participated in this test. Each subject lay in the bed for five to ten minutes with a continuous collection of the electrocardiogram (ECG). Sampling rate of the ECG is 1000Hz. Then the R-R interval series, as a function of R-peak occurrence times, were obtained by extracting the R-peaks of the ECG signal with the method of the wavelet modulus maxima[16],[17]. An example of a real R-R interval series was shown in Fig.1 (b).

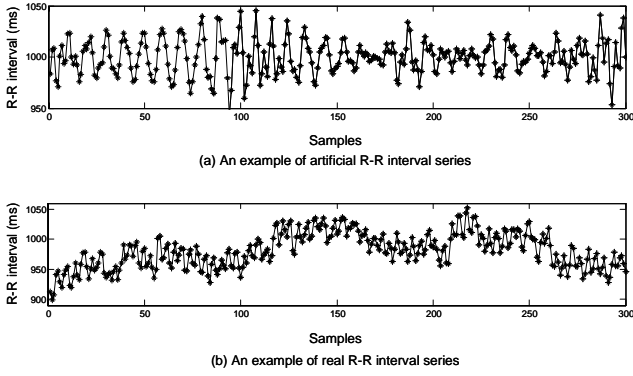


Fig. 1 Examples of artificial and real R-R interval series

C. Simulated Trends

From Fig.1 (a) we could see that there was no trend in the artificial R-R interval series. However, trends exist in almost all real R-R interval series. After an observation of hundreds of real R-R interval series, four types of trends were identified:

1. The Line Trend:

$$Line(i) = a + bi \quad (2)$$

The line trend is obtained from (2), where a is the y-intercept of the line, while b is the slope of the line.

2. The Gauss Trend:

$$Gauss(i) = Ae^{-c(i-p)^2} \quad (3)$$

The Gauss trend is generated by the Gaussian model, with appropriate settings for peak time p , sharpness c , and maximum magnitude A .

3. The Cusp Trend:

$$Cusp(i) = \sqrt{|i - a|} \quad (4)$$

The cusp trend is simulated by a cusp curve in (4), where a is the cusp point.

4. The Break Trend:

$$Break(i) = \begin{cases} A & \text{if } 0 \leq i \leq \frac{L}{2} - \frac{A}{k} \\ k\left(\frac{L}{2} - i\right) & \text{if } \frac{L}{2} - \frac{A}{k} < i < \frac{L}{2} + \frac{A}{k} \\ -A & \text{if } \frac{L}{2} + \frac{A}{k} \leq i \leq L \end{cases} \quad (5)$$

The break trend is generated from (5), with the length L , the magnitude A , and the slope k .

III. DETRENDING METHODS

A. The SPA Method

A signal, denoted as z , is considered to consist of two components[12]: $z = z_{stat} + z_{trend}$, where z_{stat} is the stationary component and z_{trend} is the trend component.

The trend component can be modeled with a linear observation model as follows,

$$z_{trend} = H\theta + v \quad (6)$$

in which, H is the observation matrix, θ are the regression parameters and v is the observation error. Then θ are estimated by the regularized least squares method,

$$\hat{\theta}_\lambda = (H^T H + \lambda^2 H^T D_d^T D_d H)^{-1} H^T z \quad (7)$$

in which, λ is the regularization parameter and D_d indicates the discrete approximation of the d 'th derivative operator. Then the estimated trend \hat{z}_{trend} is: $\hat{z}_{trend} = H\hat{\theta}_\lambda$.

With the specific choices, the identity matrix for the observation matrix H , and the second order difference matrix D_2 for D_d , the detrended signal can be written as

$$\hat{z}_{stat} = z - \hat{z}_{trend} = \left(I - (I + \lambda^2 D_2^T D_2)^{-1} \right) z \quad (8)$$

B. The Wavelet Method

The discrete wavelet transform of a signal $x(t)$ is defined as[18]:

$$\begin{aligned} D_{m,n} &= \int_{-\infty}^{+\infty} x(t) \psi_{m,n}(t) dt, \\ A_{m,n} &= \int_{-\infty}^{+\infty} x(t) \phi_{m,n}(t) dt, \end{aligned} \quad (9)$$

where $D_{m,n}$ is the detail coefficient and $A_{m,n}$ is the approximate coefficients. $\psi_{m,n}(t)$ and $\phi_{m,n}(t)$ are the dyadic grid wavelet and the scaling function, respectively.

As the trend in $x(t)$ is the approximation part, a threshold Thr is used to set the coefficients corresponding to the trend to zero, as showed in (10).

$$\hat{A}_{m,n} = \begin{cases} A_{m,n} & \text{if } A_{m,n} \geq Thr \\ 0 & \text{if } A_{m,n} < Thr \end{cases} \quad (10)$$

Then, together with $D_{m,n}$, $\hat{A}_{m,n}$ is used to reconstruct the signal. At last, we obtain the detrended signal by the inverse discrete wavelet transform as follows,

$$\hat{x}(t) = \sum_m \sum_n \hat{A}_{m,n} \phi_{m,n}(t) + \sum_m \sum_n D_{m,n} \psi_{m,n}(t) \quad (11)$$

C. The EMD Method

Given a signal $x(t)$, all the local maxima and minima are connected by a cubic spline curve as the upper envelope $e_u(t)$ and the lower envelope $e_l(t)$. Then the mean of the two envelopes is subtracted from the signal. This procedure is referred to as the sifting process[19]. The sifting process is applied repetitively until the first intrinsic mode function (IMF) $c_1(t)$ is obtained. An IMF satisfies two conditions: first, in the whole data set, the number of extrema and the number of zero

crossings must be equal or at most differed by one; and second, at any point, the mean value of the envelopes of the local maxima and minima is zero. Then, the first IMF component $c_1(t)$ is separated from $x(t)$, and we get the residue $r_1(t)=x(t)-c_1(t)$, which is treated as a new signal and applied the above procedure. Thus we can obtain other IMFs, $c_2(t)$, ..., $c_N(t)$.

The result of the decomposition produces N IMFs and a residue signal. Lower-order IMFs capture fast oscillation modes, and higher order IMFs and the residue typically represent slow oscillation modes. Thus, detrending $x(t)$ may amount to computing the partial, fine-to-coarse reconstruction

$$\hat{x}_D(t) = \sum_{n=1}^D c_n(t) \quad (12)$$

where D is the IMF index prior contaminated by the non-stationary trend.

IV. RESULTS

A. Results of Artificial R-R Interval Series

In Fig.2(a-1)~(d-1), four types of simulated trends were chosen for test, which could fall into two categories: smooth curves such as the line and Gauss trends and inflection curves such as the cusp and break trends. The four types of trends were added to the non-trend artificial R-R interval series for reconstruction of artificial R-R interval series, as shown in Fig.2(a-2)~(d-2). Then the three detrending methods were used for the reconstructed R-R interval series.

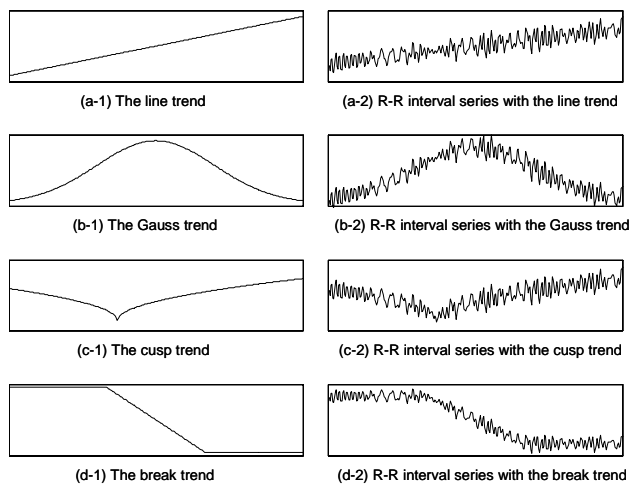


Fig. 2 Simulated trends and constructed artificial R-R interval series

The L-S periodogram was applied to assess the detrending performances. Ten thousand artificial R-R interval series were generated from McSharry's model. The parameters of the model changed randomly within a certain range, in which, f_{LF} ranged between 0.08Hz and 0.12Hz, f_{HF} ranged between 0.22Hz and 0.33Hz, and the ratio α ranged between 0.5 and 2. The theoretical values of the spectral characteristics, LF , HF , and their ratio α for each model was obtained from the artificial R-R interval series, in which, LF and HF denoted the

power of the LF and HF bands. If one of these theoretical values was I_0 , the value obtained from the R-R interval series with simulated trends or from that detrended by the SPA, wavelet(WAVE) or EMD methods was I_x , then the mean relative error was expressed as follows,

$$\bar{\delta}_x = \sum_{j=1}^N \frac{|I_x^j - I_0^j|}{I_0^j} * 100\%, N=10000. \quad (13)$$

Results were shown in Table 1. The $\bar{\delta}_{Trend}$ of LF , HF , and α were quite high. The mean relative errors of them all reduced after detrending, which showed that the trends could influence the results of spectral analysis or even cause misjudgment for HRV. Therefore, it is necessary to remove the trend before spectral analysis. The four types of trends showed different relative errors; from low to high, they were the cusp, the line, the Gauss, and the break. All trends showed higher relative errors in LF and α than in HF , which revealed that the effects of trends on different components differed. The LF band is easier to be influenced than the HF band. Moreover, the SPA method performed higher relative errors in LF of all trend models. The wavelet method and the EMD method showed excellent performance for the line and Gauss trends. But for the cusp trend, the performance of these two methods was deteriorated. In respect to the break trend, the wavelet method showed a lower relative error than the others. But the EMD method showed higher relative errors in both LF and HF than did the other methods. Thus the wavelet method showed a better overall performance than the other two methods.

For the three detrending methods, another important factor is the running speed. We compared time costs of the three methods on the artificial R-R interval series with lengths of 300, 500, 1000, 3000 and 5000, 100 ones for each length. The comparison was simulated in Matlab. As shown in Table 2, the time cost of the SPA and EMD methods increased along with the data length increased, but that of the wavelet method remained stable. The running time of the SPA method increased nonlinearly. When the length was small, the running time was short, but when the length increased to 5000, the running time increased to nearly one minute. The running time of the wavelet method was little changed as the length increased. Even when the length increased to 5000, the running time remained less than one second. Like the SPA method, the running time of the EMD method also increased with the length, but the increasing speed was lower than the SPA method. In conclusion, when the length was smaller than 500, the SPA method was more efficient than the other two, but when the length was more than 1000, the wavelet method was more efficient.

According to the simulation results, the wavelet method not only showed better detrending performance but also used less running time than did the EMD and SPA methods. Therefore, the wavelet method is recommended for detrending HRV signals, both in the short-time situation and the long-time situation.

TABLE I
MEAN RELATIVE ERRORS OF SPECTRAL ANALYSIS

		Line	Gauss	Cusp	Break
$\bar{\delta}_{Trend}$ (%)	LF	11.8±5.63	24.3±6.89	6.97±3.48	50.0±15.6
	HF	4.19±2.65	9.04±5.49	2.72±2.01	19.4±8.62
	α	8.20±5.71	15.17±9.60	5.39±3.79	27.1±16.9
$\bar{\delta}_{SPA}$ (%)	LF	1.78±0.98	1.78±0.97	1.63±1.31	1.68±1.07
	HF	0.17±0.18	0.17±0.18	0.46±0.35	0.18±0.18
	α	1.68±0.99	1.67±0.99	1.69±1.36	1.58±1.09
$\bar{\delta}_{WAVE}$ (%)	LF	0.40±0.54	0.41±0.53	1.47±1.16	0.59±0.55
	HF	0.20±0.24	0.20±0.23	0.48±0.38	0.22±0.24
	α	0.47±0.58	0.48±0.57	1.55±1.23	0.66±0.61
$\bar{\delta}_{EMD}$ (%)	LF	0.25±0.26	0.19±0.30	1.41±2.24	1.98±1.81
	HF	0.11±0.15	0.12±0.20	0.49±1.18	1.16±1.03
	α	0.28±0.29	0.24±0.31	1.41±1.21	2.05±1.84

TABLE II
RUNNING TIME OF THE DETRENDING METHODS ON DIFFERENT LENGTHS OF THE R-R INTERVAL SERIES

Length	T_{SPA} (s)	T_{WAVE} (s)	T_{EMD} (s)
300	0.12±0.02	0.41±0.05	6.20±0.58
500	0.25±0.01	0.42±0.01	7.18±0.82
1000	0.86±0.02	0.42±0.02	9.72±0.90
3000	12.30±0.53	0.42±0.01	18.96±1.77
5000	49.06±4.56	0.43±0.02	27.15±2.32

B. Results of Real R-R Interval Series

Thirty-seven healthy subjects (18 female and 19 male, Age: 55±7years; Height: 166±8cm; Weight: 66.3±10.4kg; Systolic blood pressure: 110±13mmHg; Diastolic blood pressure: 76±7mmHg; Heart rate: 66±7beats/min) participated in the real R-R interval assessment. The ECG signals were collected for 5 to 10 minutes using a cardiovascular system status monitor (CVFD-I) developed by Institute of Biomedical Engineering, Shandong University. The wavelet method was chosen to detrend the R-R interval series and the L-S periodogram was used for spectral analysis (see Table 3). Data were expressed as means±SD and compared by a paired t test with a significance level of 0.05. Statistical tests were performed with SPSS 16.0 for Windows (SPSS, Chicago, IL, USA). In Table 3, the variable change is evaluated using Δ :

$$\Delta = \frac{|X_{before} - X_{after}|}{X_{before}} * 100\%, \quad (14)$$

in which, X_{before} and X_{after} respectively denotes the spectral characteristics, LF, HF or the ratio α , of the R-R interval series before and after detrending.

TABLE III
SPECTRAL ANALYSIS OF REAL R-R INTERVAL SERIES

	LF (ms ²)	HF (ms ²)	α
Before detrending	248.37±	174.49±	1.68±1.21
After detrending	222.43	131.40	1.35±0.95
	198.28±	172.35±	
	177.13	128.67	
p	$p<0.001$	$p=0.024$	$p<0.001$
Δ (%)	19.94±5.87	1.70±2.01	18.97±5.78

The means and SD of LF, HF and the ratio α decreased after detrending, especially the LF and α ($p<0.001$). The LF and α have a change as large as about 20%, much higher than that of HF. Results of both the paired t test and the change amount indicated that the trend mainly affected the LF band of

the spectral analysis, which was consistent with the simulation results.

V. DISCUSSION

In this study, three detrending methods for spectral analysis of heart rate variability were compared. Results showed that the wavelet method performed better than the other two methods. In contrast, Wu et al. found that the EMD method is a logical choice of algorithm for extracting trends from a data set[20]. Reasons for these inconsistent results are probably because of different definition of “trends” and different gauges based. This study compared the detrending approaches using same spectral parameters whose physiological significance had been widely accepted. Considering the running speed of the three methods, the wavelet method needs less time consumption, no matter the length of HRV signals.

In previous study, usually the smooth curves, such as the line trend and the Gauss trend was used to simulate the trends[21], neglecting inflection curves like the cusp trend and the break trend in the real R-R interval series. In this study, both smooth curves and inflection curves were proposed to simulate the trends. The simulation results showed that the EMD method was appropriate to the smooth curves rather than inflection curves. However, because the real R-R interval series more commonly have trends like inflection curves; the EMD is not recommended to be used for detrending.

Table 2 showed the running time of the three methods. The calculation procedure of the SPA method involves multiplication of matrixes whose computational complexity is $O(N^3)$ [22], in which N is the data size. The time consumption of SPA will increase rapidly with prolongation of R-R interval series. The running speed of wavelet depends on computational complexity $O(N)$ [23] and decomposition level. If the decomposition level is fixed, the time cost of the wavelet method was little changed when data size increased from 300 to 5000. The computational efficiency of EMD method is

lower compared to SPA and wavelet methods, probably due to the iteration in the sifting process for IMFs decomposition. According to this study, the time consumption of the EMD method increases with prolongation of the series, higher than the other two methods.

In this study, we concentrated on the LF and HF band of the spectral analysis, so the cutoff frequency for detrending was $f < 0.04\text{Hz}$. The cutoff frequency is easy to set in the SPA and wavelet methods. For the SPA method, the cutoff frequency depends on the sampling rate of the signal and the parameter λ [12]. In the test of the artificial R-R interval series, the heart rate was set to 60, so the mean sampling rate of the series was 1Hz, thus the cutoff frequency can be easily set using the parameter λ . In this paper, we set $\lambda = 30$ and got the cutoff frequency as 0.033Hz. For the wavelet method, the cutoff frequency could be set by the decomposition level. For the mean sampling rate of the series was 1Hz, the decomposition level was set to 4 and the cutoff frequency was 0.03125Hz. As in practice the mean frequency was not fixed for different R-R interval series, the decomposition level shouldn't be fixed, too. Suppose the mean sampling rate is f_s , the decomposition level is n . A suitable level can be decided when n satisfies $f_s/2^{n+1} < 0.04\text{Hz}$. The EMD method is a data-driven method and the commonly used stopping criteria is the value of the standard deviation computed from the two consecutive sifting[19]. So the cutoff frequency of the EMD method is not fixed.

VI. CONCLUSION

In this study, comparison results of the three detrending methods, the smoothness prior approach, the wavelet and the empirical mode decomposition, showed that the wavelet method was the best choice for detrending of R-R interval series, both in short and long series. Similarly, in other physiological signal variability analysis, such as the blood pressure variability and the pulse transit time variability, similar detrending methods could be used.

ACKNOWLEDGMENT

The authors would like to thank Prof. LI Li, director of Cardiology Department of the Qilu Hospital, and Prof. YIN Jing-hai, director of Equipment Department of the Affiliated Hospital of Shandong University of Traditional Chinese Medicine, for their instructions and suggestions to this study. Authors also would like to thank all volunteers who participated in the experiments.

REFERENCES

- [1] Task Force of the European Society of Cardiology and the North American Society of Pacing and Electrophysiology, "Heart rate variability: standards of measurement, physiological interpretation and clinical use," *Circulation*, vol.93, no.5, pp. 1043-1065, 1996.
- [2] G. Berntson, J. Bigger, D. Eckberg, *et al.*, "Heart rate variability: origins, methods, and interpretive caveats," *Psychophysiology*, vol.34, no.6, pp. 623-648, 1997.
- [3] A. Rajendra, J. Paul, N. Kannathal, *et al.*, "Heart rate variability: a review," *Med Bio Eng Comput*, vol.44, no.12, pp. 1031-1051, 2006.
- [4] M. Malik and A. Camm, "Heart rate variability," *Clin Cardiol*, vol.13, no.8, pp. 570-576, 1990.
- [5] Y. Gang and M. Malik, "Heart Rate Variability: Measurements and Risk Stratification," in *Electrical Diseases of the Heart*, 1st ed. I. Gussak, C. Antzelevitch, A. Wilde, *et al.* Ed. London, Springer, 2008, pp. 365-378.
- [6] G. Clifford and L. Tarassenko, "Quantifying errors in spectral estimates of HRV due to beat replacement and resampling," *IEEE Trans Biomed Eng*, vol.52, no.4, pp. 630-638, 2005.
- [7] N. Lomb, "Least-squares frequency analysis of unequally spaced data," *Astrophys Space Sci*, vol.39, no.2, pp. 447-462, 1976.
- [8] J. Scargle, "Studies in astronomical time series analysis. II-Statistical aspects of spectral analysis of unevenly spaced data," *Astrophys J*, vol.263, pp. 835-853, 1982.
- [9] P. Laguna, G. Moody, and R. Mark, "Power spectral density of unevenly sampled data by least-square analysis: performance and application to heart rate signals," *IEEE Trans Biomed Eng*, vol.45, no.6, pp. 698-715, 1998.
- [10] D. Litvack, T. Oberlander, L. Camey, *et al.*, "Time and frequency domain methods for heart rate variability analysis: A methodological comparison," *Psychophysiology*, vol.32, no.5, pp. 492-504, 1995.
- [11] I. Mitov, "A method for assessment and processing of biomedical signals containing trend and periodic components," *Med Eng Phys*, vol.20, no.9, pp. 660-668, 1998.
- [12] M. Tarvainen, P. Ranta-aho, and P. Karjalainen, "An advanced detrending method with application to HRV analysis," *IEEE Trans Biomed Eng*, vol.49, no.2, pp. 172-175, 2002.
- [13] R. Thuraishingham, "Preprocessing RR interval time series for heart rate variability analysis and estimates of standard deviation of RR intervals," *Comput Meth Programs Biomed*, vol.83, no.1, pp. 78-82, 2006.
- [14] P. Flandrin, P. Goncalves, and G. Rilling, "Detrending and denoising with empirical mode decomposition", in *Proc. Europ Signal Process Conf.*, vol.12, 2004, pp. 1581-1584.
- [15] P. McSharry, G. Clifford, L. Tarassenko, *et al.*, "A dynamical model for generating synthetic electrocardiogram signals", *IEEE Trans Biomed Eng*, vol.50, no.3, pp. 289-294, 2003.
- [16] C. Li, C. Zheng, and C. Tai, "Detection of ECG characteristic points using wavelet transforms", *IEEE Trans Biomed Eng*, vol.42, no.1, pp. 21-28, 1995.
- [17] J. Martínez, R. Almeida, S. Olmos, *et al.*, "A wavelet-based ECG delineator: evaluation on standard databases", *IEEE Trans Biomed Eng*, vol.51, no.4, pp. 570-581, 2004.
- [18] P. Addison, "Wavelet transforms and the ECG: a review", *Physiol Meas*, vol.26, pp. R155-R199, 2005.
- [19] N. Huang, Z. Shen, S. Long, *et al.*, "The empirical mode decomposition and the Hilbert spectrum for nonlinear and non-stationary time series analysis", *Proc. Math. Physic Eng Sci*, vol.454, no.1971, pp. 903-995, 1998.
- [20] Z. Wu, N. Huang, S. Long, *et al.*, "On the trend, detrending, and variability of nonlinear and nonstationary time series". *Proc. Natl Acad Sci, USA*, vol.104, no.38, pp. 14889-14894, 2007.
- [21] K. Shafqat, S. Pal, and P. Kyriacou, "Evaluation of two detrending techniques for application in heart rate variability", in *Proc. Annu. Int. Conf. IEEE-EMBS*. Lyon, vol.29, 2007, pp. 267-270.
- [22] D. Knuth, "The Art of Computer Programming, Volume 1: Fundamental Algorithms", Addison-Wesley Professional, 1997.
- [23] H. Resnikoff and R. Wells, "Wavelet analysis: the scalable structure of information", New York: Springer-Verlag, 1998.